Available online at www.sciencedirect.com
ScienceDirect
Virology 361 (2007) 391–401
VIROLOGY
www.elsevier.com/locate/yviro

Membrane topology of murine coronavirus replicase nonstructural protein 3

Amornrat Kanjanahaluethai [a,b], Zhongbin Chen [a,c], Dalia Jukneliene [a], Susan C. Baker [a,*]

[a] *Department of Microbiology and Immunology, Loyola University of Chicago, Stritch School of Medicine, 2160 South First Avenue, Bldg. 105, Rm. 3929, Maywood, IL 60153, USA*
[b] *Department of Microbiology, Faculty of Medicine, Chiang Mai University, Chiang Mai, Thailand*
[c] *Department of Biochemistry and Molecular Biology, Beijing Institute of Radiation Medicine, Beijing, China*

Received 6 September 2006; returned to author for revision 26 September 2006; accepted 6 December 2006
Available online 12 January 2007

Abstract

Mouse hepatitis virus (MHV) is a member of the family *Coronaviridae*. These positive strand RNA viruses encode a replicase polyprotein that is processed into 16 nonstructural proteins (nsps). The nsps assemble with membranes to generate double membrane vesicles, which are the sites of viral RNA synthesis. MHV nsp3 contains multiple domains including two papain-like protease domains, PLP1 and PLP2, and a predicted transmembrane (TM) domain. In this study, we determined the membrane topology of nsp3-TM and showed that TM-mediated tethering of PLP2 is important for processing at cleavage site 3. Biochemical analysis revealed that nsp3 is an integral membrane protein that is inserted into the endoplasmic reticulum (ER) membranes co-translationally and glycosylated at asparagine-2357. Proteinase K digestion experiments indicate that the TM domain of nsp3 has 4 membrane-spanning helices. We show that nsp3-TM is sufficient in mediating ER membrane association of a cytosolic protein. This study is the first detailed analysis of the topology and function of the coronavirus nsp3 TM domain.

Keywords: Coronavirus; Replicase polyprotein; Papain-like protease; Transmembrane domain

Introduction

Proteolytic processing of a replicase polyprotein and the generation of a membrane-associated replication complex are common themes in studies analyzing the replication of positive strand RNA viruses. For the majority of coronaviruses, the proteolytic processing of the viral replicase polyprotein is mediated by three distinct viral proteinases to generate 16 replicase products [reviewed in (Ziebuhr, 2005)]. Both coronavirus and the related arterivirus replicase products have been shown to assemble with cellular membranes to generate double-membrane vesicles that are the sites of viral RNA synthesis (Goldsmith et al., 2004; Gosert et al., 2002; Pedersen et al., 1999; Snijder et al., 2006). The goal of our research is to characterize the coronavirus replicase proteolytic processing cascade and identify factors that mediate membrane-association of the replication complex.

Our model system is the replication of MHV, one of the prototype coronaviruses. MHV is a ~31.5-kilobase (kb) positive-strand RNA virus that replicates in the cytoplasm of infected cells. The 5′-most 22 kb of the MHV genomic RNA contains two large open reading frames (ORFs), termed ORF1a and ORF1b (Lee et al., 1991). During translation of the genomic RNA, the two ORFs are joined via a ribosomal frameshifting mechanism to produce a polyprotein of ~800 kilodaltons (kDa) in size (Brierley et al., 1987; Lee et al., 1991). This polyprotein is the viral RNA-dependent RNA polymerase, termed the replicase. The MHV replicase is processed by three distinct proteases contained within ORF1a of the replicase polyprotein. Two of the proteases are papain-like cysteine proteases, termed PLP1 and PLP2. The third protease domain is distantly related to the picornavirus family of 3C-like proteases, and is termed 3CLpro. These three proteases process the replicase polyprotein to produce intermediates and products that function in the replication of genomic RNA and the synthesis of a nested set of subgenomic mRNAs [reviewed in (Brian and Baric, 2005; Sawicki and Sawicki, 2005)]. Studies have shown that the replicase products alone are sufficient to mediate viral RNA synthesis (Thiel et al., 2001), and to generate

* Corresponding author. Fax: +1 708 216 9574.
E-mail address: sbaker1@lumc.edu (S.C. Baker).

0042-6822/$ - see front matter © 2006 Elsevier Inc. All rights reserved.
doi:10.1016/j.virol.2006.12.009

the double-membrane structures that serve as the sites for viral RNA synthesis (Pedersen et al., 1999). However, the role of proteolytic processing in regulating the assembly and function of the MHV replication complex is not yet understood. Therefore, we wanted to identify regions of the replicase polyprotein that may direct or regulate proteolytic processing and/or membrane association. The focus of this study was to identify the regions of MHV nsp3 that direct membrane association and PLP2 activity.

Previously, we showed the MHV PLP2 can act *in trans* to process cleavage site 3 (CS3) at the nsp3/nsp4 junction (Kanjanahaluethai and Baker, 2000; Kanjanahaluethai et al., 2003). Other coronaviruses, such as the Human Coronavirus 229E, have been shown to utilize PLP2 (also termed PL2pro) to process sites both upstream and downstream of the catalytic domain (Ziebuhr et al., 2001). The papain-like protease (PLpro) encoded by the coronavirus that causes severe acute respiratory syndrome (SARS-CoV) processes three sites in the replicase polyprotein (Harcourt et al., 2004), and has recently been shown to have de-ubiquitinating activity (Barretto et al., 2005; Lindner et al., 2005). The crystal structure of this enzyme has been resolved and is currently being targeted for anti-viral drug development (Ratia et al., 2006). A better understanding of the coronavirus papain-like proteases may facilitate anti-viral drug development for SARS and also other recently identified human coronavirus infections caused by NL63 (van der Hoek et al., 2004) and HKU1 (Woo et al., 2005), which can cause pneumonia and respiratory tract infections in children and the elderly.

The aims of this study were to determine the topology of MHV nsp3 and to identify the regions in nsp3 required for PLP2 activity. We used a *trans*-cleavage assay to determine if an expressed PLP2 domain was sufficient for the recognition and processing of a substrate containing CS3. We found that constructs containing PLP2 and the downstream putative TM domain were able to efficiently process the substrate. Bioinformatic analysis of the nsp3-TM domain indicated the presence of putative membrane-spanning helices and consensus sites for *N*-linked glycosylation. Site-directed mutagenesis of the asparagine residues and analysis of endoglycosidase H (endo H) sensitivity revealed that asparagine-2357 in nsp3-TM is glycosylated. To investigate the topology of nsp3-TM, we tested for sensitivity to digestion with proteinase K and found that at least two lumenal domains are protected, consistent with 4 membrane-spanning regions in nsp3-TM. We showed that nsp3-TM alone is sufficient to confer membrane association to a normally cytosolic protein, enhanced green fluorescent protein (EGFP), and that a predicted multi-spanning TM domain is conserved in nsp3 of all coronaviruses. Thus, the nsp3-TM domain is important for membrane association of the replicase and tethering the PLP2 domain for viral polyprotein processing activity.

Results and discussion

The MHV nsp3-TM domain is important for PLP2 processing at cleavage site 3

Analysis of SARS-CoV PLpro activity showed that the nsp3 hydrophobic domain downstream of PLpro is essential for processing at CS3 (Harcourt et al., 2004). To determine if a similar domain is important for MHV PLP2 activity, we generated a series of PLP2 C-terminal deletion constructs and tested each construct for expression and processing activity. PLP2 expression constructs were generated by polymerase chain reaction (PCR) amplification and cloning of the amplified region into pcDNA3.1/V5-His, as described in Materials and methods. To determine if each clone was expressing a protein of the expected size, we analyzed the products after T7-mediated expression and immunoprecipitation (Fuerst et al., 1986; Kanjanahaluethai and Baker, 2000). We detected the expected series of truncated PLP2 proteins that ranged in size from ~96 kDa to ~50 kDa (Fig. 1B, lanes 1–6). To determine if these PLP2 products were sufficient to mediate processing of CS3, we tested each construct in the *trans*-cleavage assay by co-transfection with the substrate (Fig. 1C, lanes 7–12). We found that only two of the PLP2 expression products, pPLP2–2485 and pPLP2–2390, were able to efficiently process the substrate and produce the 44-kDa cleavage product, nsp4 (Fig. 1C, lanes 7 and 8). These two constructs encompass all or a major part of the predicted nsp3-TM domain indicating that membrane tethering of PLP2 is important for recognition and processing at CS3. Thus, both SARS-CoV PLpro (Harcourt et al., 2004) and MHV PLP2 require the downstream TM domain for recognition and processing at the nsp3/nsp4 junction.

Bioinformatic analysis of nsp3-TM predicts a series of putative membrane-spanning sequences

Previously, we showed that MHV nsp3 is indeed an integral membrane protein, but the role of the TM in mediating this membrane association was not investigated (Gosert et al., 2002). Initial bioinformatic analysis indicated two transmembrane helices in nsp3 (Ziebuhr et al., 2001). To extend these studies of membrane association of coronavirus replicase products, we analyzed the amino acid sequence of MHV-JHM nsp3 (from glycine-833 to glycine-2840) for probability of transmembrane helices using the five different programs designed to search for putative membrane-spanning sequences: Phobius, TMHMM, HMMTOP, SOSUI and TMpred (Fig. 2). Interestingly, each program generated a unique prediction for the topology of nsp3 (Fig. 2C). The number of predicted membrane-spanning domains varied from three (Phobius) to seven (TMpred). However, since both the N- and C-termini of nsp3 are cleaved in the cytosol, the number of membrane-spanning helices must be either two [as previously predicted (Ziebuhr et al., 2001)], four or six. To better understand the topology of the nsp3-TM domain, we performed membrane-association, fractionation and proteinase K protection experiments.

Nsp3-TM is an integral membrane domain

To determine if the nsp3-TM is indeed required for membrane association, we performed in vitro transcription and translation of the PLP2 expression constructs in the absence or presence of canine microsomal membrane (CMM) and assayed for membrane association. The newly translated

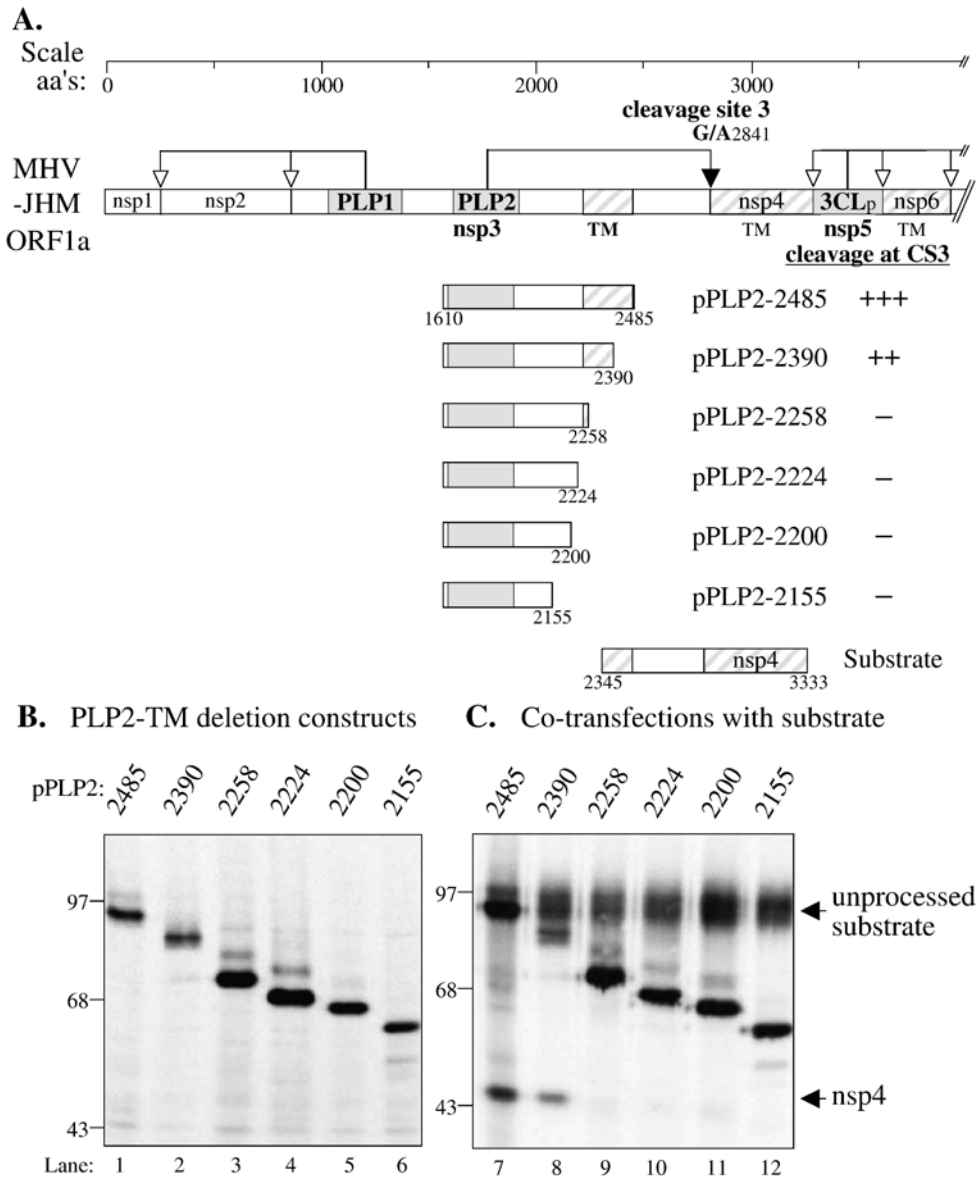

Fig. 1. (A) Schematic diagram illustrating MHV-JHM ORF1a, and the PLP2 and substrate expression constructs. MHV-JHM ORF1a containing the papain-like protease domain 1 (PLP1), the papain-like protease domain 2 (PLP2), the predicted nsp3 transmembrane domain (TM), membrane-associated nsp4, the 3C-like protease domain (3CLpro), and membrane-associated nsp6 are designated. The genetic organization and polyprotein processing of MHV-JHM ORF1a are schematically illustrated at top. Open arrows denote cleavage sites recognized by PLP1 or 3CLpro. Filled arrow indicates the cleavage site recognized by PLP2. The protease activities expressed from PLP2 constructs against the nsp3TM–nsp4 substrate are summarized: +, has *trans*-cleavage activity; −, no detectable processing of substrate. (B and C) *Trans*-cleavage activity of MHV-JHM PLP2 deletion constructs. HeLa–MHVR cells were infected with vTF7.3 and transfected with plasmid DNA encoding an MHV-JHM PLP2 region alone (B), or co-transfected with the substrate (C). Newly synthesized proteins were labeled with [^{35}S]-translabel from 5.5–10.5 hpi. Cell lysates were prepared and subjected to immunoprecipitation with anti-V5 antibody. Immunoprecipitated proteins were analyzed by electrophoresis on 5.0–12.5% gradient SDS–PAGE, processed, and subjected to autoradiography. Molecular weight markers are indicated to the left.

proteins were metabolically radiolabeled with [^{35}S]-translabel, subjected to centrifugation to separate the membrane-associated pelleted fraction from the soluble fraction. Protein products of both fractions were analyzed by sodium dodecyl sulfate–polyacrylamide gel electrophoresis (SDS–PAGE), and visualized by autoradiography (Fig. 3). The percentage of total proteins detected in soluble and pelleted fractions was quantitated by phosphoimaging analysis. In the absence of CMM, the translated protein products were detected predominantly in the soluble fraction (Fig. 3A). In contrast, when CMMs were added to the mixture, protein products that included all or part of nsp3-TM (PLP2–2485, –2390 and –2258) were detected predominantly in the pelleted fraction, consistent with membrane association (Fig. 3B). To determine if the membrane association occurred co-translationally or post-translationally, we added the CMMs after termination of translation, and assessed membrane association. Previous studies with hepatitis C virus revealed post-translational insertion of the NS5A replicase protein (Brass et al., 2002). We found that the translation product of PLP2–2485 is inserted co-translationally,

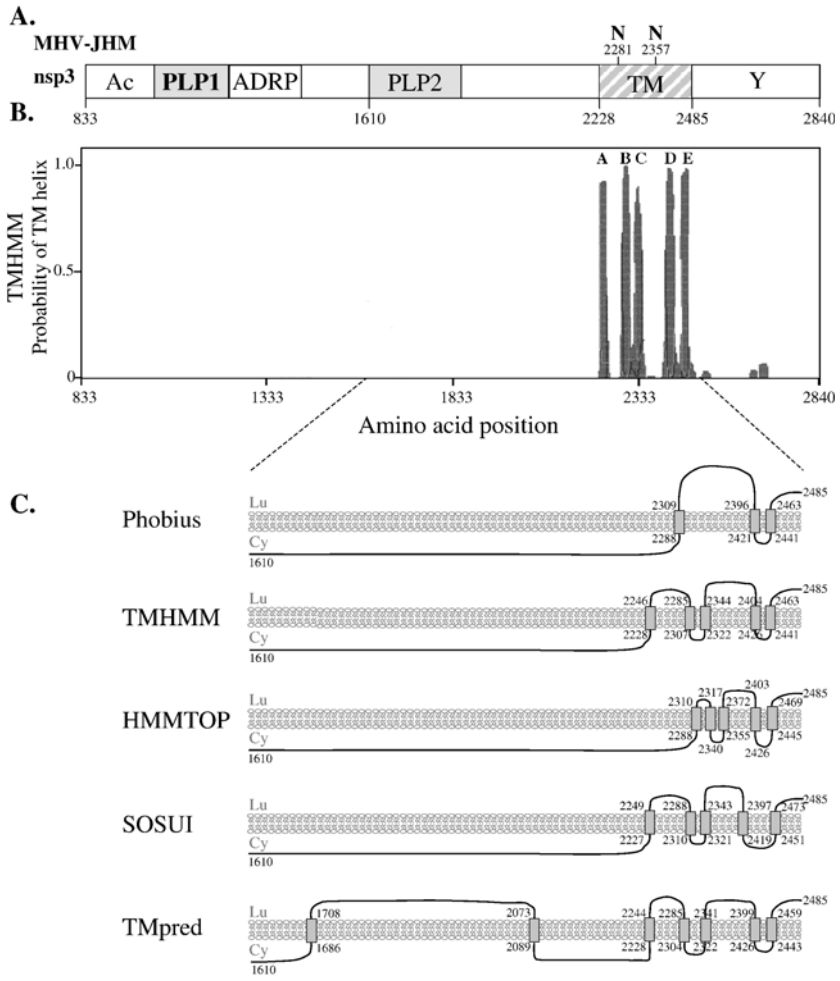

Fig. 2. Diagram of the probability of transmembrane helices in MHV-JHM nsp3. (A) The MHV-JHM nsp3 extends from amino acid glycine-833 to glycine-2840. The amino acid numbering is according to NCBI accession number NC006852. Conserved domains previously identified by comparative sequence analysis (Ziebuhr et al., 2001) and the recently described ADP-ribose-1″-phosphatase (ADRP) domain (Saikatendu et al., 2005) are indicated. Two putative sites for *N*-linked glycosylation were predicted at asparagine residues 2281 and 2357. (B) The diagram shows the results of an analysis of the nsp3 for predicted transmembrane helices using TMHMM program. The predicted TM domain designates the boundaries of the putative membrane-spanning regions A, B, C, D, and E. (C) Sequence of the PLP2–TM (amino acid residues 1610 to 2485) were analyzed for the prediction of transmembrane domains using Phobius, TMHMM, HMMTOP, SOSUI and TMpred programs.

with no detectable post-translational insertion into membranes (Fig. 3C). These results indicate that MHV nsp3 membrane insertion likely occurs via the normal, signal recognition particle (SRP)-dependent ER translocation mechanism, and not via a tail-anchoring or post-translational mechanism.

To distinguish between membrane association versus integral membrane insertion, membrane extraction experiments were performed. Protein products expressed from pPLP2–2485, pPLP2–2390 and pPLP2–2258 constructs were translated in vitro in the presence of CMM and the pelleted fraction was subsequently subjected to differential extraction methods as indicated in Fig. 4. As expected, treatment with NTE buffer alone had no effect and the proteins pelleted with membranes, whereas treatment with detergent Triton X-100 disrupted the membranes, and the proteins were detected in the soluble fraction (Fig. 4A). Treatments with urea, NaCl or sodium carbonate, pH 11.5 have been shown to disrupt the association between peripheral, membrane-associated proteins, but such treatments do not disrupt integral membrane proteins (Bordier, 1981). We tested for disruption of PLP2–TM proteins and found that majority of the proteins remained in the pelleted membrane fraction, consistent with integral membrane proteins (Fig. 4B). We noted that the protein product expressed from pPLP2–2258, which contains only one or two predicted membrane spanning helices, was dissociated by treatment with high pH, but that the protein products expressed from constructs that extended further into the TM were not disrupted from the membranes by these treatments, consistent with the characteristics of integral membrane proteins.

Bioinformatic analysis also revealed two consensus sequences for *N*-linked glycosylation [the consensus being NX(T/S), where X is any amino acid (Helenius and Aebi, 2001)] in nsp3-TM. If one or more of the predicted sequences was indeed a transmembrane helix, then the sites for *N*-linked glycosylation could be lumenal, and subject to modification. To determine if either of the putative sites was modified by glycosylation, we

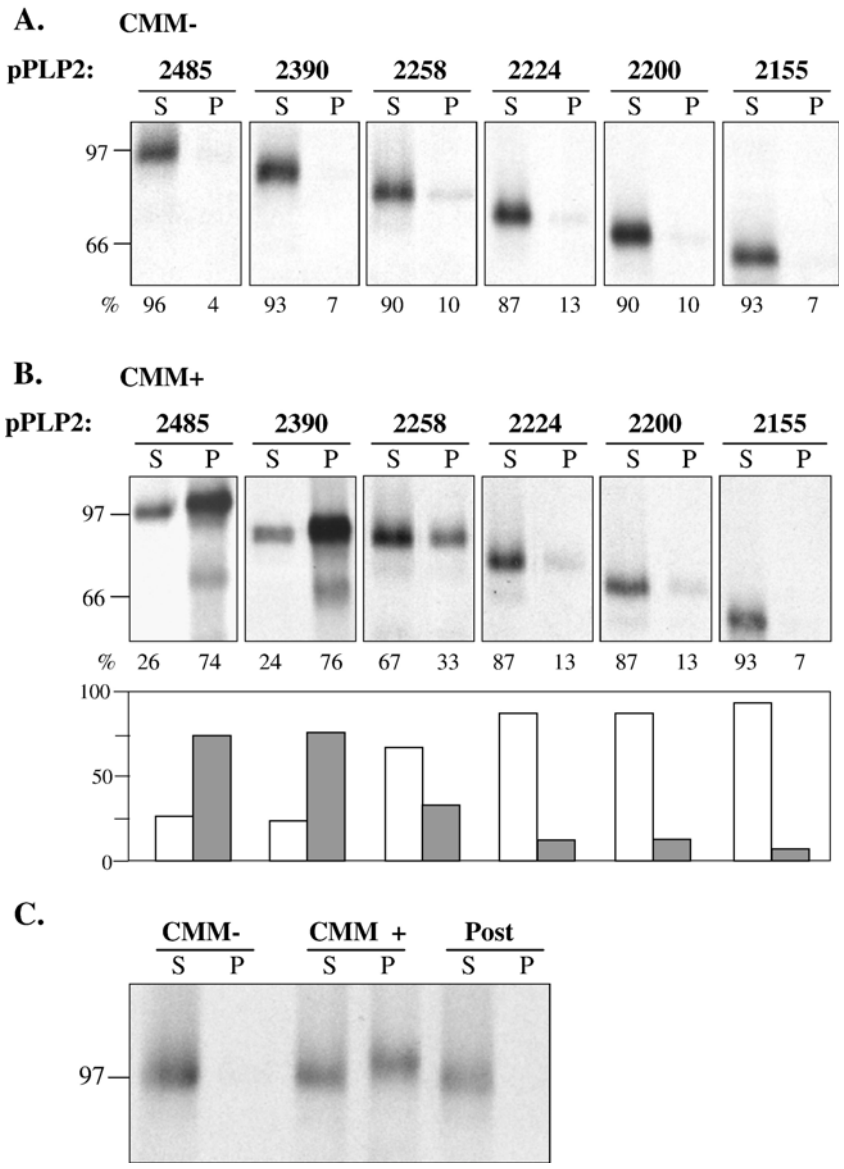

Fig. 3. Detection of membrane association of the MHV-JHM PLP2 expressed protein products. Plasmid DNAs were linearized and subjected to in vitro transcription and translation in the absence (A) or presence (B) of CMM, or post-translational addition of CMM (C). Proteins were labeled with [^{35}S]-translabel, immunoprecipitated with anti-V5 antibody, analyzed on 10% SDS–PAGE, visualized by autoradiography, and quantitated by phosphoimaging. The percentages of total protein detected in the soluble (S) versus the pelleted (P) fraction are indicated below the gel. White bars represent proteins detected in soluble fraction, while gray bars represent proteins detected in pellet fraction.

subjected the proteins expressed from wild-type pPLP2–Cen (Kanjanahaluethai and Baker, 2000) and two asparagine-to-alanine substitution mutants to endo H treatment (Fig. 5). Expressed proteins were radiolabeled with [^{35}S]-translabel, lysates were prepared, and subjected to immunoprecipitation with anti-V5 antibody as described in Materials and methods. The PLP2–Cen protein was either untreated, or treated with endo H for 16 h, then analyzed for mobility by electrophoresis through a 5% polyacrylamide gel. We found that the untreated wild-type protein migrated at approximately 110 kDa (lane 1). However, after digestion with endo H, the protein migrated at 108 kDa (lane 2), consistent with the loss of one *N*-linked modification. The PLP2–Cen–N2357A protein with an asparagine-to-alanine substitution migrated more quickly than the wild type or N2281A protein, indicating that N2357 is the site modified by *N*-linked glycosylation (compare lanes 3–5). Furthermore, proteins generated by endo H treatment of the pPLP2–Cen–N2357A and pPLP2–Cen–N2281A migrated more quickly than wild type PLP2–Cen (lanes 6–8). These results indicate that nsp3 is glycosylated at asparagine-2357. Overall, these experiments demonstrate that nsp3-TM does have transmembrane and lumen sequences that can tether the PLP2 domain to intracellular membranes.

To further investigate the topology of nsp3-TM, we tested for sensitivity to proteinase K digestion. Cytosolic domains are sensitive to proteinase K, whereas transmembrane and lumenal domains are protected from digestion with proteinase K. Analysis of PLP2–2485 revealed two major fragments of

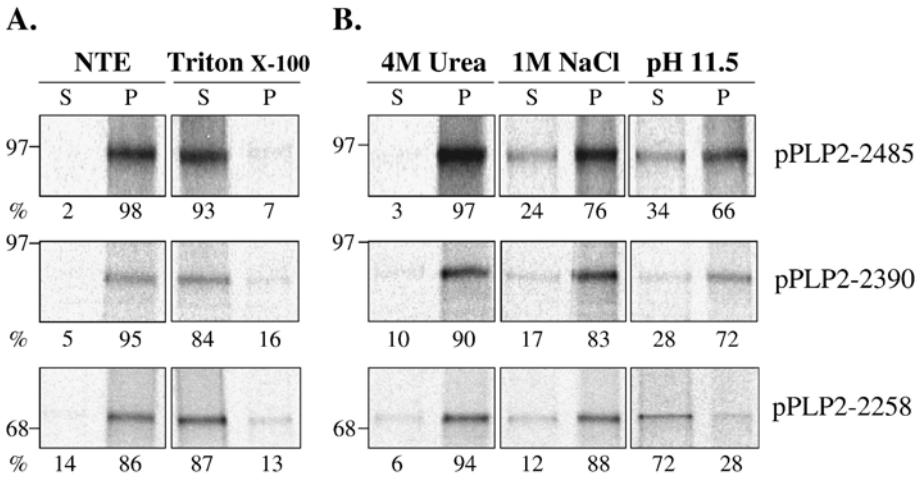

Fig. 4. Membrane extraction experiments of the PLP2 expressed protein products treated with Triton X-100, urea, NaCl or sodium carbonate solution pH 11.5. In vitro transcription and translation reactions of pPLP2–2485, pPLP2–2390 or pPLP2–2258 were performed in the presence of CMM. Subsequently, reaction mixtures were centrifuged to sediment CMM containing associated PLP2 protein. The supernatant were removed and the pellets were resuspended in NTE buffer or 0.5% Triton X-100 (A), 4 M urea, 1 M NaCl or 100 mM sodium carbonate solution pH 11.5 (B) and incubated for 20 min at 4 °C. Subsequently, membrane sedimentation analyses were performed as described under Materials and methods. Soluble (S) and pellet (P) fractions were applied in equivalent amounts and subjected to 12% SDS–PAGE analysis. Quantitation was performed by phosphoimaging and values expressed in % were given at the bottom and depicted as bars.

28 kDa and 10 kDa protected from proteinase K digestion (Fig. 6, lane 2). We noted the predicted size of the TM domain from K2227-Y2469 is 28.0 kDa, and the predicted size of the K2227-I2308 (A and B helices) is 9.6 kDa. Analysis of PLP2–2390 revealed two protected fragments of 19 kDa and 10 kDa, respectively (Fig. 6, lane 4). The predicted size of the K2227-S2390 fragment is 18.8 kDa. By combining the results of the integral membrane assays (Figs. 3 and 4), the glycosylation assay (Fig. 5), and the proteinase K sensitivity assay (Fig. 6A), we were able to generate a topology model for nsp3-TM that is consistent with all the data (Figs. 6B and C). Our results indicate that nsp3-TM has four membrane-spanning sequences and two lumenal domains (Fig. 6B) and that the 10 kDa fragment likely represents the proteinase K resistant fragment generated by the first two membrane-spanning sequences. Our model is most similar to the predicted models generated by the TMHMM and SOSUI programs with the exception that the fourth predicted membrane-spanning sequence (which is the only domain not consistent in these two predictions) is not a membrane-spanning sequence, but instead remains lumenal, and the final membrane-spanning domain is in the reverse orientation. Our results, and the results of others (Hugle et al., 2001; Miller et al., 2006), demonstrate the importance of experimental validation of bioinformatics predictions of membrane-spanning sequences. For example, in the case of Dengue virus type 2 nonstructural protein 4B, Miller and co-workers found that two computer-predicted transmembrane helices were in fact lumenal and one was glycosylated (Miller et al., 2006). In addition, we note the value of using multiple programs to better estimate the complexity of the bioinformatic prediction. The differences in the predicted models could then be tested experimentally. Here, we provide an initial model of nsp3-TM that should be refined by further experimentation. Similar studies should also be performed to determine the topology of nsp4 and nsp6, the other coronavirus replicase products with multiple predicted transmembrane helices.

Finally, to determine if the TM domain of MHV nsp3 was sufficient to confer membrane association to a cytosolic protein, we appended nsp3-TM to EGFP and determined the localization of the fusion protein using confocal microscopy (Fig. 7). EGFP normally is distributed throughout the cell (Fig. 7A). We found that appending the MHV nsp3-TM sequence to EGFP

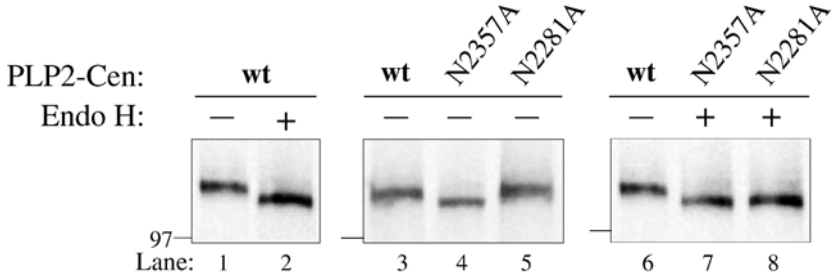

Fig. 5. Effect of amino acid substitution of asparagine residue 2281 or 2357 on the migration of the PLP2–Cen protein. Asparagine residue 2281 or 2357 was changed to an alanine residue by site-directed mutagenesis as described in Materials and methods. Wild-type and mutant plasmid DNAs were expressed via the vaccinia virus–T7 expression system, and immunoprecipitated products were analyzed by electrophoresis on 10% SDS–PAGE. The effect of treatment with endo H to remove *N*-linked glycosylation is shown.

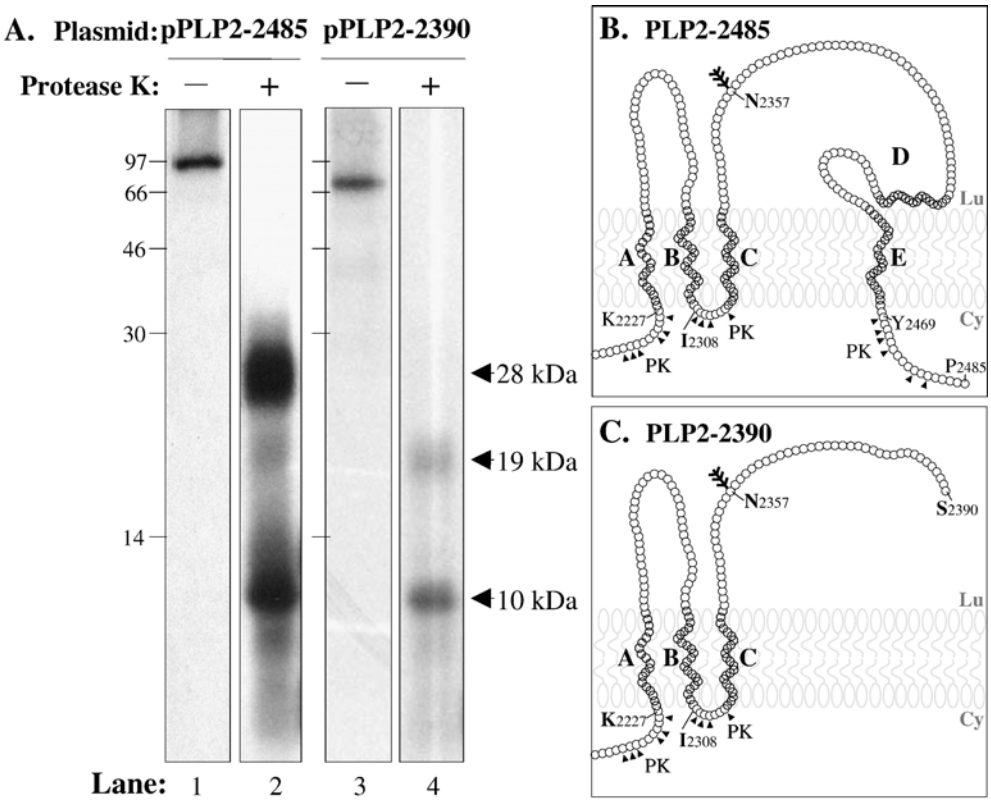

Fig. 6. Digestion of the PLP2–TM translation products with proteinase K. Cell-free transcription and translation assay of either linearized pPLP2–2485 or pPLP2–2390 in the presence of CMM were performed as described in Materials and methods. Proteins were labeled with [^{35}S]-translabel for 90 min, and then treated with proteinase K for 30 min. The digested products were analyzed on 15% SDS–PAGE, and subjected to autoradiography. (B) The proposed model of proteinase K protection to PLP2–2485 translation product. Arrowheads depict potential proteinase K cleavage sites. The tree symbol (🌲) represents the experimentally confirmed *N*-linked glycosylation site of asparagine at position 2357. The putative membrane-spanning regions A, B, C, D, and E of the nsp3 TM domain are depicted by gray circles. (C) The proposed model of PK protection of PLP2–2390 translation product.

was sufficient to tether it to membranes, as shown by the intense, perinuclear localized signal (Fig. 7B). To determine if the nsp3-TM domain is retained in the ER membranes or is transported through the medial Golgi, we radiolabeled the EFGP–nsp3TM protein in transfected cells, immunoprecipitated the protein and subjected the immunoprecipitated products to endo H. We found that EFGP–nsp3TM is sensitive to treatment with endo H, indicating that the protein is retained in the ER and does not pass through the medial Golgi. Thus, the nsp3-TM domain is sufficient to confer membrane-localization and retention in the ER. These studies are in agreement with our previous findings showing that the TM domain of SARS-CoV nsp3 (previously termed the HD) confers membrane association of EGFP (Harcourt et al., 2004).

In summary, using biochemical fractionation and proteinase K protection assays, we show that nsp3-TM likely has four membrane-spanning domains, and that lumenal residue asparagine-2357 is modified by glycosylation. Furthermore, we found the region nsp3-TM domain is required for efficient MHV PLP2 process activity at cleavage site 3 in the polyprotein. Why does MHV PLP2 require membrane association for proteolytic processing of the PLP2 cleavage site? One possible explanation is that membrane-tethering brings PLP2 into close proximity with a membrane-associated substrate. It is also possible that the nsp3-TM membrane tether is important for anchoring the replicase complex to intracellular membranes. Bioinformatic analysis of the nsp3 of 10 other coronaviruses revealed that the membrane-spanning features of nsp3-TM are conserved in all viruses (Fig. 8, analysis using the TMHMM program is shown as an example), even though the amino acid identity is relatively low (18–32% identity within nsp3). Therefore, the TM domain is likely to be important for both PLP2 activity and assembly of the replication complex. Further studies will be required to determine the precise topology of the TM domain in other coronaviruses, and if the lumenal sequences in nsp3-TM play any role in interacting with host factors during viral replication.

Materials and methods

Cells

HeLa cells expressing the MHV receptor, HeLa–MHVR cells (Gallagher, 1996) were used for all transfection experiments. The cells were grown in Dulbecco's modified Eagle's medium supplemented with 10% fetal bovine serum (Invitrogen, Carlsbad, CA), 0.5% penicillin/streptomycin, 2% glutamine, and 5 mM sodium *N*-2-hydroxyethylpiperazine-*N*′-2-ethanesulfonic acid, pH 7.4.

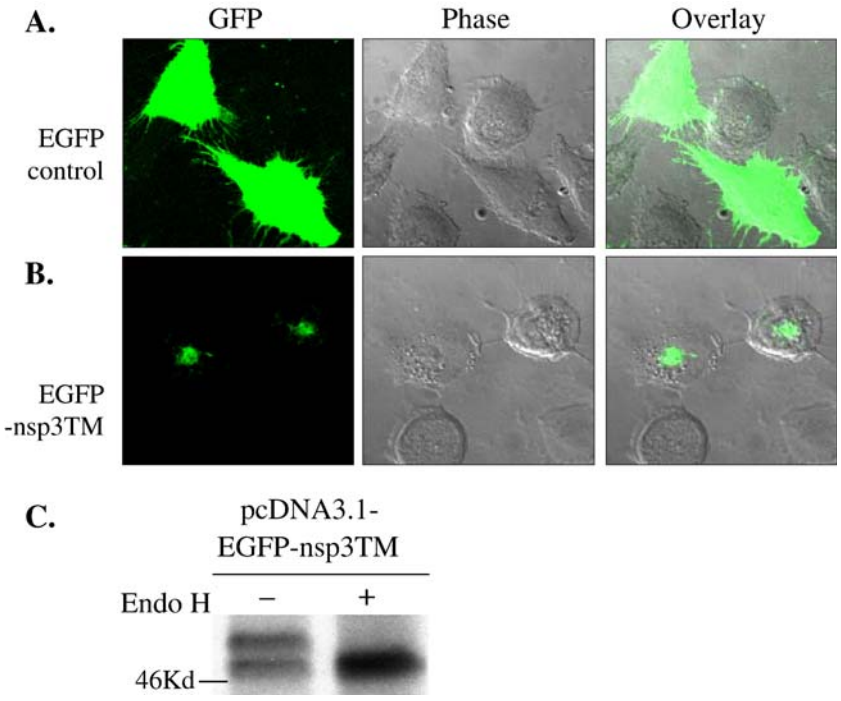

Fig. 7. Detection of EGFP from transfected cells. HeLa–MHVR cells were transfected with either pEGFP (A) or pEGFP–nsp3TM (MHV-JHM amino acid alanine-2228 to valine-2478) (B) for 48 h. Then cells were washed, and visualized by confocal microscopy. (C) EFGP–nsp3TM was cloned into the pcDNAV5His expression vector and plasmid DNA was expressed via the vaccinia virus–T7 expression system and immunoprecipitated with anti-V5. Immunoprecipitated products were incubated in the presence or absence of endo H and analyzed by electrophoresis on 10% SDS–PAGE.

Construction of MHV-JHM PLP2 expression plasmids

Recombinant plasmid DNA constructs expressing the PLP2 coding region were generated using specific primers (listed in Table 1) to amplify the designated region from the parental plasmid pPLP2–Cen (Kanjanahaluethai and Baker, 2000). The region of interest was generated by PCR amplification using LA-*Taq* polymerase according to the manufacturer's instructions (Clontech, Palo Alto, CA). The amplified region was then digested with restriction enzymes *Bam*HI and *Xho*I and ligated into the corresponding sites in the pcDNA3.1/V5-His expression vector (Stratagene, La Jolla, CA) using T4 ligase (New England Biolabs). The ligated DNA product was transformed into XL-1 Blue competent cells according to the manufacturer's instructions (Stratagene), except that the bacteria were grown at 25 °C.

PLP2 trans-cleavage assay

HeLa–MHVR cells were infected with a recombinant vaccinia virus expressing the bacteriophage T7 polymerase (vTF7-3) at a multiplicity of infection of 10. Then, infected cells were co-transfected with recombinant plasmid DNAs encoding the MHV-JHM indicated protease domain and the substrate using lipofectamine according to manufacturer's instruction as previously described (Fuerst et al., 1986; Kanjanahaluethai and Baker, 2000). Newly synthesized proteins were metabolically labeled with 50 μCi/ml [^{35}S]-translabel (ICN, Costa Mesa, CA) from 5.5 to 10.5 h post-infection (hpi). To harvest the cells, radioactive labeled cells were washed with phosphate buffered saline (PBS), and cell lysates were prepared by scraping the cells in lysis buffer A [4% SDS, 3% DTT, 40% glycerol and 0.065 M Tris, pH 6.8 (Schiller et al., 1998)]. The lysates were either used directly for immunoprecipitation assays or stored at −70 °C for future studies.

Radioimmunoprecipitation assays

Radiolabeled cell lysate was diluted in 1.0 ml RIPA buffer [0.5% Triton X-100, 0.1% SDS, 300 mM NaCl, 4 mM EDTA, and 50 mM Tris–HCl, pH 7.4 (Schiller et al., 1998)] and subjected to immunoprecipitation with anti-V5 monoclonal antibody (Invitrogen) and protein-A sepharose beads (Amersham Biosciences, Piscataway, NJ). The immunoprecipitated products were eluted with 2× Laemmli sample buffer, incubated at 30 °C for 30 min, and analyzed by electrophoresis on a 5.0–12.5% gradient polyacrylamide gel containing 0.1% SDS. Following electrophoresis, the gel was fixed in 25% methanol–10% acetic acid, enhanced with Amplify (Amersham Biosciences) for 60 min, dried, and exposed to Kodak X-ray film at −70 °C.

Site-directed mutagenesis of putative glycosylation sites in MHV-JHM nsp3-TM domain

Plasmid DNA pPLP2–Cen which encompasses MHV-JHM gene 1 amino acid residues 1525–2485 (Kanjanahaluethai and Baker, 2000) was subjected to site-directed mutagenesis at positions 7055 and 7056 for pPLP2–N2281A and positions

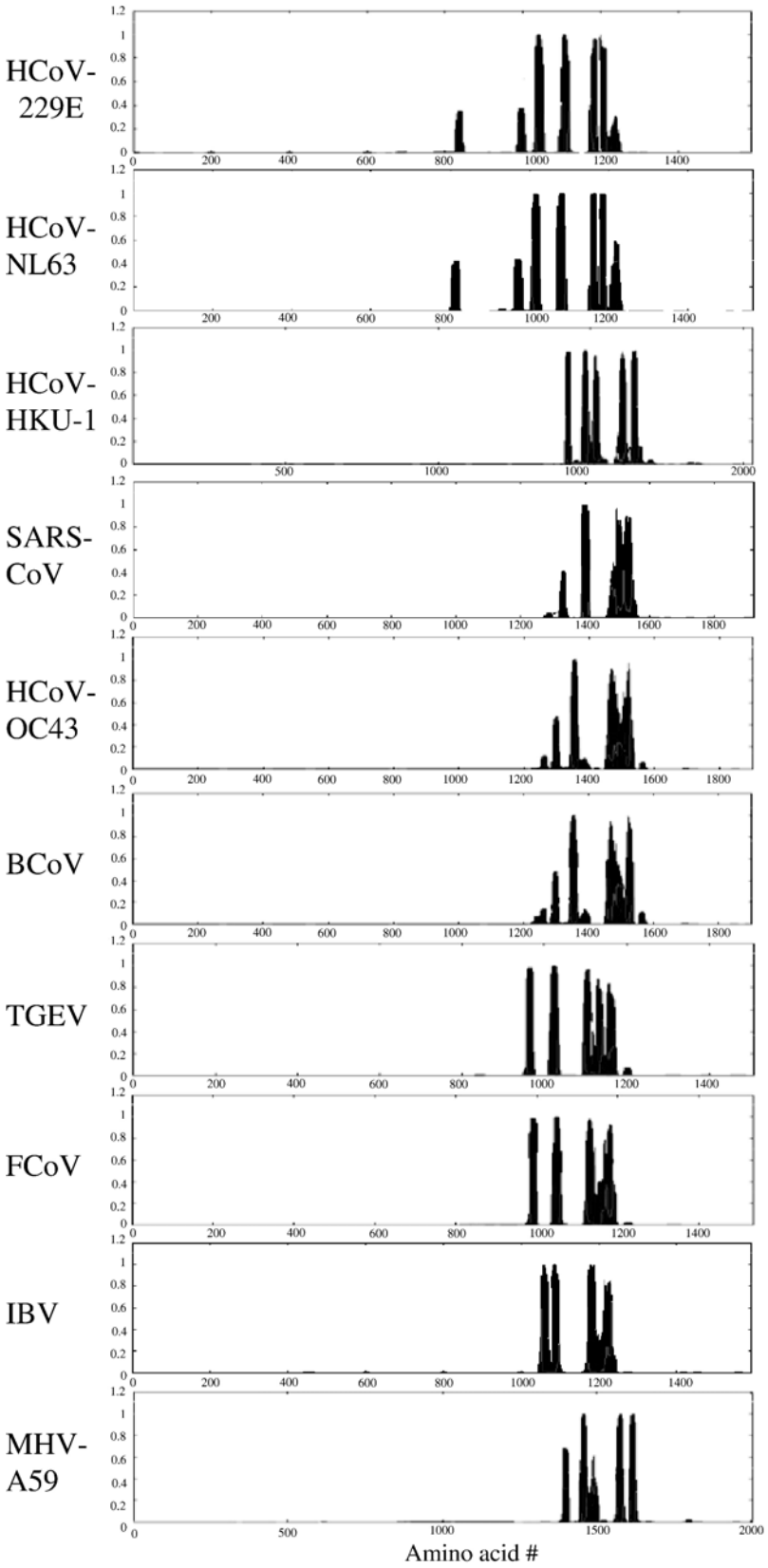

Fig. 8. Diagram of the probability analysis of transmembrane helix domains in nsp3 of 10 coronaviruses using the TMHMM program. NCBI accession numbers are as follows: Human coronavirus (HCoV) 229E, NC_002645 (nt 2984–7744); HCoV-NL63, NC_005831 (nt 2981–7672); HCoV-HKU1, NC006577 (nt 2633–8719); SARS-CoV (Urbani), AY278741 (nt 2719–8484); HCoV-OC43, NC_005147 (nt 2764–8460); bovine coronavirus (BCoV), NC_003045 (nt 2764–8460); transmissible gastroenteritis virus of pigs (TGEV), NC_002306 (nt 2952–7478); feline coronavirus (FCoV), AY994055 (nt 2948–7549); infectious bronchitis virus of chickens (IBV), NC_001451 (nt 2548–7323); murine coronavirus strain MHV-A59, NC_001846 (nt 2706–8720). All these coronavirus genomes are available at the NIH sponsored *Pat*hogen *R*esource *I*ntegration *C*enter, PATRIC, at www.patric.vbi.vt.edu.

Table 1
Primers used for amplification or mutagenesis of MHV-JHM sequences

Construct name	Primer	Oligonucleotide sequence (5′ to 3′)[a]	Nucleotide number[b]	Polarity
pPLP2–2485	B244	GGGGATCCAGGATGGTTGATGTCTTGTGTA	5042–5057	Forward
	B205	CCCTCGAGCCAGGCTTACTACATCCATA	7652–7671	Reverse
pPLP2–2390	B258	AACTCGAGGACACACGCCTATCTAC	7367–7383	Reverse
pPLP2–2258	B345	TTCTCGAGGCTTTCGCTTTGACCAC	6881–6897	Reverse
pPLP2–2224	B346	GCCTCGAGGACATACCCCACTTAAC	6797–6813	Reverse
pPLP2–2200	B327	GGCTCGAGACTTCTGTGGTGTATAT	6977–6993	Reverse
pPLP2–2155	B257	GGCTCGAGACTTTGGTTTCGCTAGTG	6661–6678	Reverse
pEGFP–nsp3TM	B410	AACTCGAGCTATTGCCTGCTTAG	6896–6911	Forward
	B411	AAGGATCCAACATGTCTACAAAGACAATAGAC	7625–7648	Reverse
pcEGFP–nsp3TM	ZCP1	AAGGATCCGTCGCCACCATGGTGAGCAAGGGC	EGFP	Forward
	ZCP2	AATCTAGACTAACATGTCTACAAAGACAATAGAC	7625–7648	Reverse
	Site-directed mutants[c]			Amino acid changed
B341	GAATGCCTTACAGACGTTTGCTTGGAGCGTTG TGTCTAGGGG		7036–7077	N2281A
B343	GGCTATAGGAGTTCGTTTTGTGCTGGAAGTATGGTCTGTGAAC		7262–7304	N2357A

[a] Underlined sequences were required for cloning, expression of MHV sequences or mutagenesis.
[b] MHV-JHM nucleotide numbers are according to NCBI accession number NC006852.
[c] Sequence of one primer of each complementary primer pair is shown.

7283 and 7284 for pPLP2–N2357A using synthetic oligonucleotides with mismatches encoding specific nucleotides changes as shown in Table 1. Mutagenesis was performed according to the manufacturer's instructions (QuickChange Site-Directed Mutagenesis; Stratagene), and as previously described (Kanjanahaluethai and Baker, 2000). Mutations were confirmed by DNA sequence analysis.

In vitro transcription and translation

The TNT T7-coupled reticulocyte lysate system (Promega, Madison, WI) was used according to the manufacturer's instructions. The recombinant plasmid DNA encoding the designated PLP2 region was linearized by digestion with *Pme*I. In vitro transcription and translation was performed for 90 min at 30 °C in the presence of 0.8 μCi of [^{35}S]-translabel per ml in a volume of 25 μl. Where indicated, 1.0 μl of CMM (Promega) was added prior to the incubation. For analysis of membrane association, the products of in vitro transcription and translation were centrifuged at 14,000 rpm for 10 min. The supernatant was removed, the pellet that may contain aggregated or membrane-associated protein was suspended in 2× Laemmli sample buffer, heated at 95 °C for 5 min, and both fractions were analyzed by SDS–PAGE and subjected to autoradiography.

Proteinase K protection assay

Protection of translation products by microsomal membranes was examined by digestion with proteinase K (Hugle et al., 2001). Following translation, reaction mixtures (after incubation with RNase A) were adjusted to 0.5 mg/ml of proteinase K (Roche, Indianapolis, IN) and incubated for 30 min on ice. Proteinase K digestion was terminated by addition of phenylmethylsulfonyl fluoride to 1 mg/ml and incubation was continued for 5 min on ice. A portion of each reaction mixture (generally 4 μl) was mixed with 40 μl of 2× Laemmli sample buffer, heated at 95 °C for 5 min, analyzed by 15% SDS–PAGE and subjected to autoradiography.

Endoglycosidase H treatment

For endo H treatment, lysates from vTF7.3-infected and pPLP2–TM transfected cells were prepared and subjected to immunoprecipitation as described above. Protein-A sepharose–antibody–antigen complexes were washed once in RIPA buffer and endo H treatment was performed as suggested by the manufacturer (Roche). Briefly, the complexes were resuspended in 20 μl of 50 mM sodium phosphate buffer, pH 6.0, and incubated in the presence or absence of a final concentration of 1 unit/μl of endo H for 16 h at 37 °C. Following the incubation, 25 μl of 2× Laemmli sample buffer was added to each sample, mixed, and incubated for 30 min at 37 °C. The sepharose beads were pelleted by a brief, high-speed spin in a microfuge, and the supernatant loaded directly for analysis by 12% SDS–PAGE and subjected to autoradiography.

Determining membrane association

For membrane extraction experiments, the pellets from 15 μl in vitro transcription–translation reactions performed in the presence of CMM were resuspended in 40 μl NTE buffer, 0.5% Triton X-100, 4 M urea, 1 M NaCl, or 100 mM sodium carbonate (pH 11.5) and incubated for 20 min at 4 °C (Hugle et al., 2001). Subsequently, supernatant and pellet fractions were separated by centrifugation at 14,000 rpm for 10 min, and analyzed by SDS–PAGE and autoradiography. Quantitation was performed by using phosphoimaging analysis.

Expression of EGFP–nsp3TM

The putative transmembrane domain 1 region of MHV-JHM nsp3 (nt 6896 to 7648) was PCR amplified from the pPLP2–Cen (Kanjanahaluethai and Baker, 2000) with primers B410

and B411 (Table 1), cloned into the mammalian expression vector for EGFP, pEGFP-C1 (BD Biosciences), and designated pEGFP–nsp3TM. The plasmid DNA encoding EGFP or EGFP–nsp3TM was transfected into HeLa–MHVR cells in 8-well chamber culture slides with lipofectamine according to manufacturer's instructions, for 48 h. Expression of EGFP and EGFP–nsp3TM fusion protein products was detected by confocal microscopy (Zeiss LSM 510 lazer-scanning confocal microscope). EGFP–nsp3TM was amplified by primers ZCP1 and ZCP2 (Table 1) using pEGFP–nsp3TM as template, and then cloned into *Bam*HI and *Xba*I sites of pcDNA3.1/V5-HisB (Invitrogen) to generate the construct of pcDNA3.1–EGFP–nsp3TM. The plasmid DNA was expressed via the vaccinia virus–T7 expression system, proteins radiolabeled with ^{35}S-translabel, cell lysates were subjected to immunoprecipitation with anti-V5 antibody, and products were either incubated with endo H or buffer alone, and analyzed by electrophoresis on 10% SDS–PAGE.

Acknowledgments

We thank Nicole Kreuziger, Kari Severson and Ami Knop Ullrich for excellent technical assistance, and Dr. Alexander Gorbalenya, Leiden University Medical Center for useful suggestions during the course of this work. This research was supported by Public Health Service Research Grants AI 45798 and HHSN2662040035C.

References

Barretto, N., Jukneliene, D., Ratia, K., Chen, Z., Mesecar, A.D., Baker, S.C., 2005. The papain-like protease of severe acute respiratory syndrome coronavirus has deubiquitinating activity. J. Virol. 79 (24), 15189–15198.

Bordier, C., 1981. Phase separation of integral membrane proteins in Triton X-114 solution. J. Biol. Chem. 256 (4), 1604–1607.

Brass, V., Bieck, E., Montserret, R., Wolk, B., Hellings, J.A., Blum, H.E., Penin, F., Moradpour, D., 2002. An amino-terminal amphipathic alpha-helix mediates membrane association of the hepatitis C virus nonstructural protein 5A. J. Biol. Chem. 277 (10), 8130–8139.

Brian, D.A., Baric, R.S., 2005. Coronavirus genome structure and replication. Curr. Top. Microbiol. Immunol. 287, 1–30.

Brierley, I., Boursnell, M.E., Binns, M.M., Bilimoria, B., Blok, V.C., Brown, T.D., Inglis, S.C., 1987. An efficient ribosomal frame-shifting signal in the polymerase-encoding region of the coronavirus IBV. EMBO J. 6 (12), 3779–3785.

Fuerst, T.R., Niles, E.G., Studier, F.W., Moss, B., 1986. Eukaryotic transient-expression system based on recombinant vaccinia virus that synthesizes bacteriophage T7 RNA polymerase. Proc. Natl. Acad. Sci. U.S.A. 83 (21), 8122–8126.

Gallagher, T.M., 1996. Murine coronavirus membrane fusion is blocked by modification of thiols buried within the spike protein. J. Virol. 70 (7), 4683–4690.

Goldsmith, C.S., Tatti, K.M., Ksiazek, T.G., Rollin, P.E., Comer, J.A., Lee, W.W., Rota, P.A., Bankamp, B., Bellini, W.J., Zaki, S.R., 2004. Ultrastructural characterization of SARS coronavirus. Emerg. Infect. Dis. 10 (2), 320–326.

Gosert, R., Kanjanahaluethai, A., Egger, D., Bienz, K., Baker, S.C., 2002. RNA replication of mouse hepatitis virus takes place at double-membrane vesicles. J. Virol. 76 (8), 3697–3708.

Harcourt, B.H., Jukneliene, D., Kanjanahaluethai, A., Bechill, J., Severson, K.M., Smith, C.M., Rota, P.A., Baker, S.C., 2004. Identification of severe acute respiratory syndrome coronavirus replicase products and characterization of papain-like protease activity. J. Virol. 78 (24), 13600–13612.

Helenius, A., Aebi, M., 2001. Intracellular functions of *N*-linked glycans. Science 291 (5512), 2364–2369.

Hugle, T., Fehrmann, F., Bieck, E., Kohara, M., Krausslich, H.G., Rice, C.M., Blum, H.E., Moradpour, D., 2001. The hepatitis C virus nonstructural protein 4B is an integral endoplasmic reticulum membrane protein. Virology 284 (1), 70–81.

Kanjanahaluethai, A., Baker, S.C., 2000. Identification of mouse hepatitis virus papain-like proteinase 2 activity. J. Virol. 74 (17), 7911–7921.

Kanjanahaluethai, A., Jukneliene, D., Baker, S.C., 2003. Identification of the murine coronavirus MP1 cleavage site recognized by papain-like proteinase 2. J. Virol. 77 (13), 7376–7382.

Lee, H.J., Shieh, C.K., Gorbalenya, A.E., Koonin, E.V., La Monica, N., Tuler, J., Bagdzhadzhyan, A., Lai, M.M., 1991. The complete sequence (22 kilobases) of murine coronavirus gene 1 encoding the putative proteases and RNA polymerase. Virology 180 (2), 567–582.

Lindner, H.A., Fotouhi-Ardakani, N., Lytvyn, V., Lachance, P., Sulea, T., Menard, R., 2005. The papain-like protease from the severe acute respiratory syndrome coronavirus is a deubiquitinating enzyme. J. Virol. 79 (24), 15199–15208.

Miller, S., Sparacio, S., Bartenschlager, R., 2006. Subcellular localization and membrane topology of the dengue virus type 2 non-structural protein 4B. J. Biol. Chem. 281 (13), 8854–8863.

Pedersen, K.W., van der Meer, Y., Roos, N., Snijder, E.J., 1999. Open reading frame 1a-encoded subunits of the arterivirus replicase induce endoplasmic reticulum-derived double-membrane vesicles which carry the viral replication complex. J. Virol. 73 (3), 2016–2026.

Ratia, K., Saikatendu, K.S., Santarsiero, B.D., Barretto, N., Baker, S.C., Stevens, R.C., Mesecar, A.D., 2006. Severe acute respiratory syndrome coronavirus papain-like protease: structure of a viral deubiquitinating enzyme. Proc. Natl. Acad. Sci. U.S.A. 103 (15), 5717–5722.

Saikatendu, K.S., Joseph, J.S., Subramanian, V., Clayton, T., Griffith, M., Moy, K., Velasquez, J., Neuman, B.W., Buchmeier, M.J., Stevens, R.C., Kuhn, P., 2005. Structural basis of severe acute respiratory syndrome coronavirus ADP-ribose-1″-phosphate dephosphorylation by a conserved domain of nsP3. Structure (Camb) 13 (11), 1665–1675.

Sawicki, S.G., Sawicki, D.L., 2005. Coronavirus transcription: a perspective. Curr. Top. Microbiol. Immunol. 287, 31–55.

Schiller, J.J., Kanjanahaluethai, A., Baker, S.C., 1998. Processing of the coronavirus MHV-JHM polymerase polyprotein: identification of precursors and proteolytic products spanning 400 kilodaltons of ORF1a. Virology 242 (2), 288–302.

Snijder, E.J., van der Meer, Y., Zevenhoven-Dobbe, J., Onderwater, J.J., van der Meulen, J., Koerten, H.K., Mommaas, A.M., 2006. Ultrastructure and origin of membrane vesicles associated with the severe acute respiratory syndrome coronavirus replication complex. J. Virol. 80 (12), 5927–5940.

Thiel, V., Herold, J., Schelle, B., Siddell, S.G., 2001. Viral replicase gene products suffice for coronavirus discontinuous transcription. J. Virol. 75 (14), 6676–6681.

van der Hoek, L., Pyrc, K., Jebbink, M.F., Vermeulen-Oost, W., Berkhout, R.J., Wolthers, K.C., Wertheim-van Dillen, P.M., Kaandorp, J., Spaargaren, J., Berkhout, B., 2004. Identification of a new human coronavirus. Nat. Med. 10 (4), 368–373.

Woo, P.C., Lau, S.K., Chu, C.M., Chan, K.H., Tsoi, H.W., Huang, Y., Wong, B.H., Poon, R.W., Cai, J.J., Luk, W.K., Poon, L.L., Wong, S.S., Guan, Y., Peiris, J.S., Yuen, K.Y., 2005. Characterization and complete genome sequence of a novel coronavirus, coronavirus HKU1, from patients with pneumonia. J. Virol. 79 (2), 884–895.

Ziebuhr, J., 2005. The coronavirus replicase. Curr. Top. Microbiol. Immunol. 287, 57–94.

Ziebuhr, J., Thiel, V., Gorbalenya, A.E., 2001. The autocatalytic release of a putative RNA virus transcription factor from its polyprotein precursor involves two paralogous papain-like proteases that cleave the same peptide bond. J. Biol. Chem. 276 (35), 33220–33232.